Available online at www.sciencedirect.com
SCIENCE DIRECT®
Renewable Energy 30 (2005) 1177–1194
RENEWABLE ENERGY
www.elsevier.com/locate/renene

Theoretical approach of a flat plate solar collector with clear and low-iron glass covers taking into account the spectral absorption and emission within glass covers layer

Maatouk Khoukhi*, Shigenao Maruyama

Institute of Fluid Science, Tohoku University, Katahira 2-1-1, Aoba-ku, Sendai 980-8577, Japan

Received 8 September 2003; accepted 23 September 2004
Available online 2 December 2004

Abstract

Accurate modeling of solar collector system using a rigorous radiative model is applied for the glass cover which represents the most important component of the system and greatly affects the thermal performance. The glass material is analyzed as a non-gray plane-parallel medium subjected to solar and thermal irradiations in one dimensional case using the radiation element method by ray emission model (REM^2). The optical constants of a clear and low-iron glass materials proposed by Rubin have been used. These optical constants, 160 values of real part n and imaginary part k of the complex refractive index of such materials, cover the range of interest for calculating the solar and thermal radiative transfer through the glass cover. The computational times for predicting the thermal behavior of solar collector were found to be prohibitively long for the non-gray calculation using 160 values of n and k for both glasses. Therefore, suitable semi-gray models have been proposed for rapid calculation. The temperature distribution within the glass cover shows a good agreement with that obtained with iterative method in case of clear glass. It has been shown that the effect of the non-linearity of the radiative heat exchange between the black plate absorber and the surroundings on the shape of the efficiency curve is important. Indeed, the thermal loss coefficient is not constant but is a function of temperature, due primarily to the radiative transfer effects. Therefore, when the heat exchange by radiation is dominant compared with the convective mode,

* Corresponding author. Tel./fax: +81 22 217 5244.
E-mail address: kmaatouk@pixy.ifs.tohoku.ac.jp (M. Khoukhi).

doi:10.1016/j.renene.2004.09.014

the profile of the efficiency curve is not linear. It has been also shown that the instantaneous efficiency of the solar collector is higher in case of low-iron glass cover.

Keywords: Flat-plate solar collector; Glass cover; Optical constants; Non-gray; Semi-gray; Efficiency; CPU time

1. Introduction

The thermal analysis of solar collectors is still difficult, even though the theoretical simplified approach has been available for many decades [1,2]. The accurate prediction of the thermal performance of solar collector system depends strongly on how the glass cover material is analyzed.

In this paper, a classical flat plate solar collector with black absorbing surface is considered. The glass cover is treated as a participating non-gray medium subjected to solar radiation, specified by the spectral solar model for cloudless atmosphere proposed by Bird and Riordan [3], and thermal radiation emanating from the black absorber and from the outside environment which are also assumed to be black. The absorption and emission within the glass cover are taken into account using 160 values of the optical constant, real part n and imaginary part k of the complex refractive index of clear and low-iron glasses proposed by Rubin [4], covering the range of solar and thermal radiation (0.3–300 μm). The boundary surfaces of the glass cover are specular and the spectral dependence of the radiation properties is all taken into consideration.

A more refined and rigorous approach is applied using radiation element method by ray emission model (REM^2) [5,6]. The back and lateral heat losses are assumed to be negligible. The system was simulated by varying the mean black plate absorber temperature.

The calculation has been performed for one position of the sun chosen at noon on the first of February in Sendai City (Japan). The temperature distributions within the glass covers and steady heat fluxes through the glasses layers have been obtained. Using non-gray models (NG) with 160 bandwidths (NG160b), the CPU times were found to be prohibitively long, around 17 h on personal computer (VT-Alpha 600, 21164A, 600 MHz) for both cases, clear and low-iron glasses. Hence, simplified semi-gray models (SG) have been proposed. Steady state heat fluxes and temperature distributions within the glass covers have been calculated in case of SG models and compared with those obtained when using NG models.

2. Theoretical models

The important parts of a typical flat plate solar collector as shown in Fig. 1 are: the black solar energy-absorbing surface, with means for transferring the absorbed energy to a fluid; a glass cover which reduces convection and radiation losses to the atmosphere; and back and lateral insulation to reduce the conduction losses as the geometry of system

Nomenclature

A_i^R	effective radiation area, m^2
c_p	specific heat, J kg^{-1}
e_{air}	thickness of the air layer between the glass and the plate absorber, m
f	parameter defined in Eq. (21)
$F_{i,j}^A$	absorption view factor from element i to j
$G_{i,\lambda}$	incident radiation, W m^{-2}
Gr	Grashoff number, dimensionless
h_{in}	inside convective heat transfer coefficient, W K^{-1} m^{-2}
h_{out}	outside convective heat transfer coefficient, W K^{-1} m^{-2}
$h_{r,p-g}$	radiation coefficient from the plate to the glass cover, W m^{-2} C^{-1}
$h_{r,g-s}$	radiation coefficient from the cover to the sky, W m^{-2} C^{-1}
I	global solar irradiation on the collector area, W m^{-2}
k	imaginary part of the complex refractive index of the glass cover
n	real part of the complex refractive index of the glass cover
Nu	Nusselt number, dimensionless
$Q_{J,i,\lambda}$	heat transfer rate of diffuse radiosity, W
$Q_{T,i,\lambda}$	heat transfer rate of emissive power, W
$Q_{x,i,\lambda}$	net heat transfer rate of heat generation, W
$q_{r,\lambda}$	radiative heat flux, W m^{-2}
$q_{x,i}$	net rate of heat generation per unit volume or unit surface, W m^{-3}, W m^{-2}
S_h	heat source, W m^{-3}
T_i	temperature of element i, K
T_{abs}	absorber temperature, K
$T_o(nl)$	absorber-side glass temperature, K
T_{air}	temperature of the air layer between the glass cover and the absorber, K
T_g	mean glass cover temperature, K
T_p	black plate absorber temperature, K
T_{amb}	ambient temperature, K
T_s	sky temperature, K
U_t	overall heat transfer coefficient, W m^{-2} K^{-1}
V	wind speed, m s^{-1}
V_i	volume of volume element or surface area of surface element, m^3, m^2

Greek letters

α	absorptivity of the black absorber
β	slope of the solar collector, degrees
Δx_i	element thickness, m
ε	emissivity
Λ_g	thermal conductivity of the glass cover, W m^{-1} K^{-1}
ρ_g	density of the glass cover, kg m^{-3}
σ	Stefan–Boltzmann constant, W m^{-2} K^{-4}
τ_g	transmissivity of the glass cover
Ω_i^D	albedo of the volume element or diffuse of surface element

Subscripts

abs	absorber
amb	ambient
g	glass cover
i	element *i*
j	element *j*
p	plate absorber
s	sky
λ	spectral value

permits. In the present study, the back and lateral conduction losses are assumed to be negligible.

2.1. Radiation transfer through the glass cover

Fig. 2 shows the model of solar collector glass-cover used in the present study. The solar collector glazing is subjected to collimated direct solar and diffuse solar and thermal irradiations. It is assumed that the glazing unit exists between two blackbodies which comprise the ambience of the surroundings and the air between the plate black absorber and the glass cover. The analysis is carried out by dividing the glazing into a number of elements. Since the long-wavelength radiation from the ambient is mostly absorbed in the vicinity of the glass surface, the thickness of the element is thin (1 μm) at the glass surface and thick (200 μm) in the middle of the glass. The total number of element is set at 103. We assume that each radiation element is at constant uniform temperature, and the real part of the complex refractive index n and heat generation rate per unit volume are also

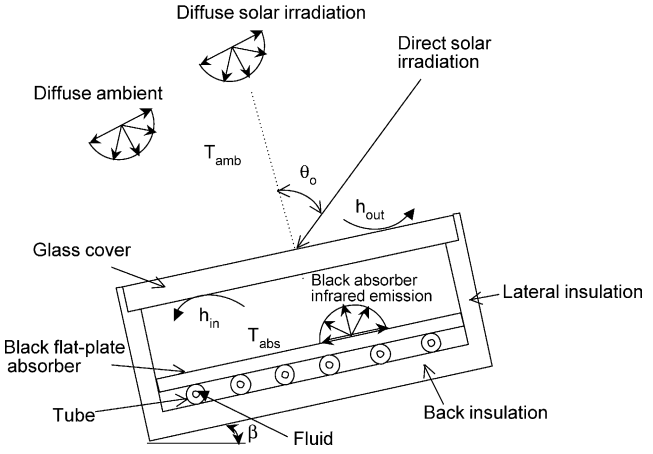

Fig. 1. Flat-plate solar collector subjected to the solar and thermal irradiations.

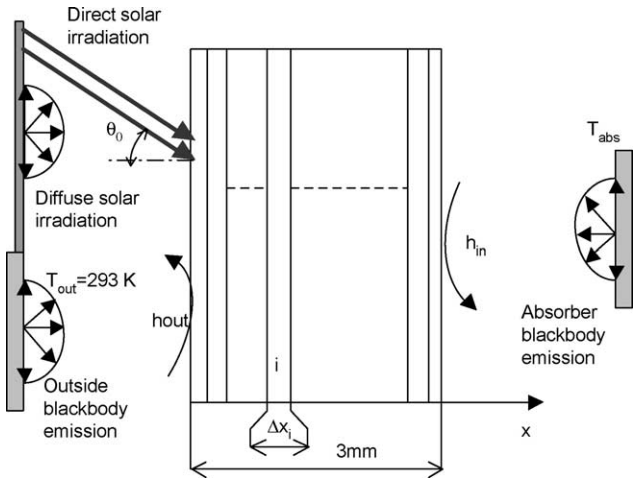

Fig. 2. Analysis model of solar collector glass cover.

constant and uniform throughout the element. The scattering is neglected and the thermal conductivity of the glass is assumed to be constant.

The rate at which radiation energy is emitted by the radiation element is given by the following expression [5,6]

$$Q_{J,i,\lambda} = A_i^{\mathrm{R}}(\varepsilon_i n^2 \sigma T_i^4 + \Omega_i^{\mathrm{D}} G_{i,\lambda}) \tag{1}$$

where ε_i, n, σ and T_i are the glass emissivity, real part of the complex refractive index of the glass cover, Stefan–Boltzman constant and temperature, respectively. Ω_i^{D} is the albedo of the volume element or diffuse of surface element as defined by [5,6] and $G_{i,\lambda}$ is the spectral irradiance on radiation element i. A_i^{R} is the effective radiation area [5,6].

The net rate of heat generation can be derived from the heat balance on the radiation element [5,6]

$$Q_{X,i,\lambda} = A_i^{\mathrm{R}} \varepsilon_i (n^2 \sigma T_i^4 - G_{i,\lambda}) \tag{2}$$

As it was mentioned, the scattering is neglected $\Omega_i^{\mathrm{D}} = 0$, therefore, the heat transfer rate of diffuse radiosity $Q_{J,i,\lambda}$ is equal to the heat transfer rate of emissive power defined as follows [5,6]

$$Q_{T,i,\lambda} = A_i^{\mathrm{R}} \varepsilon_i n^2 \sigma T_i^4 \tag{3}$$

If the system is consisted of N volume and surface elements ($N-2$ participating layers and two boundary surfaces), Eqs. (1) and (2) can be rewritten as [5,6]

$$\begin{aligned} Q_{J,i,\lambda} &= Q_{T,i,\lambda} \\ Q_{X,i,\lambda} &= Q_{T,i,\lambda} - \sum_{j=1}^{N} F_{j,i}^{\mathrm{A}} Q_{J,i,\lambda} \end{aligned} \tag{4}$$

in which, the absorption view factor $F_{j,i}^{\mathrm{A}}$ is introduced as defined by Maruyama and Aihara [5,6]. The heat transfer rate of spectral emissive power $Q_{T,i,\lambda}$ or the net rate of heat

generation $Q_{x,i,\lambda}$ for each radiation element is given as a boundary condition [5,6]. The unknown $Q_{T,i,\lambda}$ or $Q_{x,i,\lambda}$ can be obtained by solving Eq. (4).

The total net rate of heat generation is given by

$$Q_{X,i} = \int_0^\infty Q_{X,i,\lambda}\, \mathrm{d}\lambda \tag{5}$$

The heat generation rate of the radiation per unit volume or unit surface area is expressed as

$$q_{x,i} = Q_{X,i}/V_i \tag{6}$$

where V_i is the volume of volume element or surface area of surface element.

The radiation heat flux through the layer is derived as [5,6]

$$q_{r,\lambda}(x) = q_{X,1} + \sum_{i=2}^{n}(q_{X,\lambda,i}\Delta x_i) \tag{7}$$

$q_{x,1}$ includes the blackbody emission emanating from the ambient, and the diffuse and direct solar radiation components, Δx_i is the element thickness (see Fig. 2).

2.2. Convective heat transfer coefficients

The convection is taken into account at both sides of the glass cover assuming the outside convective heat transfer coefficient h_{out} in term of wind speed calculated using the empirical equation proposed by Watmuff and reported by Agarwal and Larson [7]

$$h_{\mathrm{out}} = 2.8 + 3V \tag{8}$$

where V is the wind speed close to collector in m s^{-1}.

The convective heat transfer coefficient between the glass and absorber, h_{in}, is evaluated using the equations expressed by Duffie and Beckman [1], assuming the natural convection of the air between two parallel planes

$$h_{\mathrm{in}} = \frac{Nu\Lambda_{\mathrm{air}}}{e_{\mathrm{air}}} \tag{9}$$

Λ_{air} and e_{air} are the thermal conductivity and the thickness of the air layer between the glass and the absorber, respectively.

The Nusselt number is given by the following relation

$$Nu = [0.06 - 0.017(\beta/90)]Gr^{1/3} \tag{10}$$

β is the solar collector tilt angle in degrees.

The Prandtl number is included in the above equation and assumed to be independent of temperature and taken equal to 0.7 [1].

The Grashoff number is

$$Gr = \frac{g|T_{\mathrm{abs}} - T_{\mathrm{o}}(\mathrm{nl})|e_{\mathrm{air}}^3}{\nu^2 T_{\mathrm{air}}} \tag{11}$$

Table 1
Data used to compute h_{in}

Parameter	Symbols	Value	Unit
Prandlt number	Pr	0.7	–
Thickness of the air layer between the glass and the absorber plate	e_{air}	0.04	m
Thermal conductivity of the air layer	Λ_{air}	0.028 (average value)	$W\,m^{-1}\,K^{-1}$
Kinematic viscosity of the air layer	ν	19.5×10^{-6} (average value)	$m^2\,s^{-1}$
Slope of the collector	β	40	degrees

T_{abs} and T_o(nl) are the absorber temperature and the absorber-side of glass temperature, respectively. T_{air} is assumed to be equal to the average temperature between the flat absorber and the absorber-side glass cover. The data used in the present study to compute h_{in} is given in Table 1.

The one-dimensional unsteady conductive heat transfer through the glass layer is given by

$$\rho c_p \frac{\partial T}{\partial t} = \Lambda_g \frac{\partial^2 T}{\partial x^2} + S_h \tag{12}$$

where ρ, c_p, Λ_g, t and S_h are the density of the glass, specific heat of the glass, thermal conductivity of the glass, time and the heat generation source, respectively.

2.3. Classical approach

In order to compare the present method with the conventional approaches, a classical approach is adopted. In the classical approach, the analysis of the performance of the collector begins by writing energy balances on the cover for an assumed temperature of the absorber, and solving for the cover temperature [2]. As will be seen, this requires an iterative solution. In the analysis to follow, it is assumed: the surfaces are gray for the infrared; the cover is opaque for the infrared. The radiation coefficient from the black plate absorber to the glass is [1]

$$h_{r,p-g} = \frac{\sigma(T_p^2 + T_g^2)(T_p + T_g)}{\varepsilon_p^{-1} + \varepsilon_g^{-1} - 1} \tag{13}$$

where σ, T_p, T_g, ε_p and ε_g are Stefan–Boltzman constant, black plate absorber temperature, glass cover temperature, plate absorber emissivity (0.95) and glass cover emissivity (0.88) [2], respectively. The radiation coefficient from the cover to the sky is given by

$$h_{r,g-s} = \varepsilon_g \sigma(T_g^2 + T_s^2)(T_g + T_s) \tag{14}$$

The sky temperature T_s is related to the ambient temperature by the following relation given by Swinbank [1]

$$T_s = 0.0552 T_{amb}^{1.5} \tag{15}$$

where T_s and T_{amb} are both in Kelvin.

The outside and inside convective heat transfer coefficients, h_{out} and h_{in}, are the same as in Eqs. (8) and (9), respectively, except for Grashoff number (Eq. (11)) $T_o(nl)$ is substituted by the average glass temperature T_g. The overall heat loss coefficient of the solar collector, neglecting the back and lateral heat losses, is given by the following relation

$$U_t = \{(h_{in} + h_{r,p-g})^{-1} + (h_{out} + h_{r,g-s})^{-1}\}^{-1} \tag{16}$$

The cover temperature is found by noting that the heat loss from the plate to the cover is the same as from the plate to the surroundings neglecting the absorption of the radiation energy by the glass cover, as well as its thermal capacity, therefore

$$T_g = T_p - \frac{U(T_p - T_{amb})}{h_{in} + h_{r,p-g}} \tag{17}$$

The procedure is to guess a cover temperature from which all the heat transfer coefficients are calculated and the top loss coefficient is also evaluated. These results are then used to calculate T_g from the above equation. If T_g is close to the initial guess, no further calculation are necessary. Otherwise, the newly calculated T_g is used and the process is repeated.

The instantaneous efficiency of the solar collector for a unit area of the collector is [1,2]

$$\eta = (\tau\alpha)_{eff} - \frac{U_t(T_{abs} - T_{amb})}{I} \tag{18}$$

$(\tau\alpha)_{eff}$ is the effective absorptance of the cover glass-absorber assembly and given by the following relation

$$(\tau\alpha)_{eff} = \frac{\alpha\tau_g}{1 - (1 - \alpha)\rho_g} \tag{19}$$

in which, α, τ_g and ρ_g are the absortivity of the black absorber, the transmittance of the glass cover and the reflectance of the glass cover calculated by Fresnel equations [2], respectively.

The top heat loss coefficient U_t is evaluated using Klein model [2] and given by the following expression

$$U_t = \left[\frac{1}{\left(\frac{344}{T_p}\right)\left[\frac{(T_p - T_{amb})}{(1+f)}\right]^{0.31}} + h_{out}^{-1}\right]^{-1} + \frac{\sigma(T_p + T_{amb})(T_p^2 + T_{amb}^2)}{[\varepsilon_p + 0.0425(1 - \varepsilon_p)]^{-1} + \left[\frac{(1+f)}{\varepsilon_g}\right] - 1} \tag{20}$$

with

$$f = 1.058(1 - 0.04h_{out} + 0.0005h_{out}^2) \tag{21}$$

3. Results and discussion

The calculation has been carried out for one location at noon on the first of February in Sendai City (Japan). The site characteristics and other parameters used in calculation are

Table 2
Characteristics of the site and other parameters used in numerical simulation

Parameter	Value	Unit
Zenith angle (ζ)	55.47	degrees
Latitude	38.16	degrees
Longitude	140.51	degrees
Altitude	45.0	m
Day of year	32	–
Wind speed velocity	1.5	m/s
Ambient temperature	293	K

given in Table 2. The solar collector is simulated in steady state varying the mean absorber plate temperature.

Fig. 3 shows the spectral variation of the optical constants, real part n and imaginary part k of the complex refractive index, of clear and low-iron glasses commonly used as covers for solar collector. Each model contains 160 bandwidths (NGCL160b and NGLI160b for a clear and low-iron glasses, respectively) covering the range of interest from the visible to the far infrared. These values have been reported by Rubin using Kramer–Kronigs Formulates [4]. The curve of the real part n shows two peaks around 10 and 22 μm, and the curve of imaginary part k shows two bands of strong absorption around 9.5 and 21 μm which affect the heat flux and the temperature distribution within a glass cover. The curves of the real part n of the complex refractive index are similar for both clear and low-iron glasses. Low-iron glass, which contains less iron oxides in the raw materials, produce less absorption in the visible and near infrared (0.3–5 μm). Indeed, the curve of k for low-iron glass is smaller than that for clear glass in the range of 0.3–5 μm. On the other hand, k values are the same for clear and low-iron glasses in the infrared range.

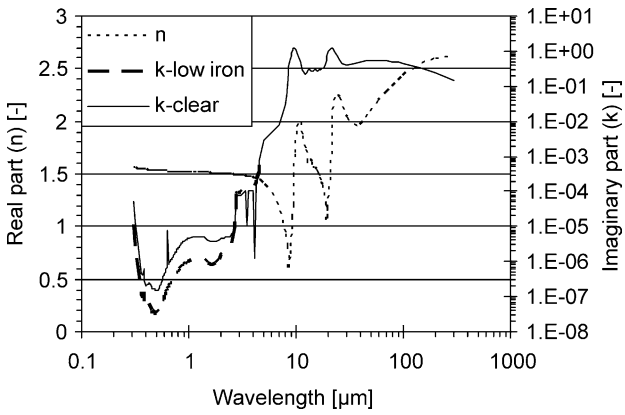

Fig. 3. Real part (n) and imaginary part (k) of the complex refractive index of clear and low-iron glasses, non-gray models.

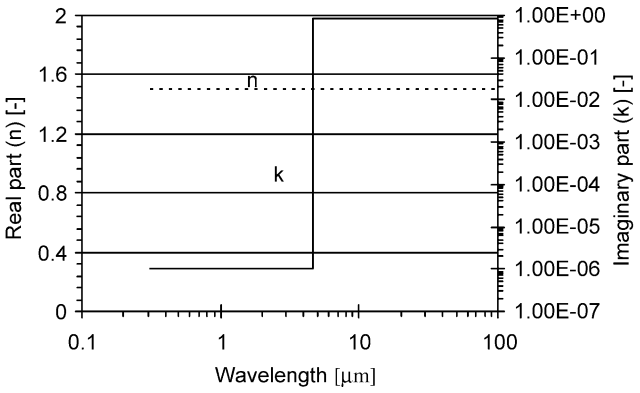

Fig. 4. Real part (n) and imaginary part (k) of the complex refractive index of clear glass cover, semi-gray model.

3.1. Clear glass

The solar collector system has been simulated using NG model of n and k. The CPU time consumed was found to be prohibitively long. Therefore, a simplified semi-gray model (SGCL), in which the spectral nature of radiation heat transfer in collector is modeled by two spectral bands, is proposed for a rapid calculation. Fig. 4 shows the optical constants of clear glass (SGCL model).

The CPU time, steady heat flux and temperature distribution are obtained in case of SGCL model and compared with those obtained with the reference model NGCL160b. The validation of SGCL model has been done for two values of the average temperature of the absorber T_{abs} at 40 °C (low temperature) and 80 °C (high temperature).

Fig. 5 shows the steady heat flux through the glass cover layer obtained both with non-gray and semi-gray models at 40 °C and 80 °C of T_{abs}. The steady heat flux obtained in

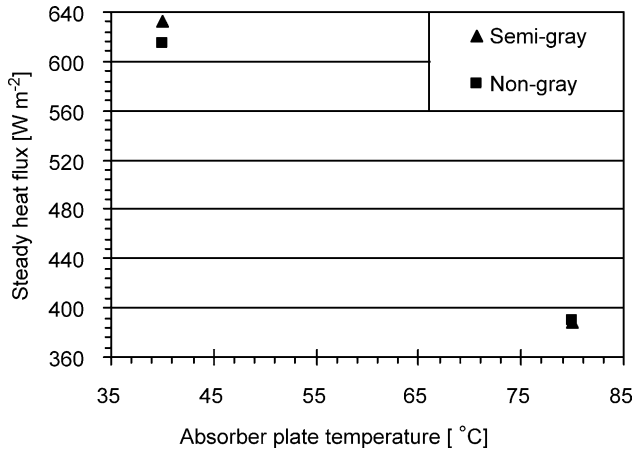

Fig. 5. Steady heat fluxes through the clear glass cover using non-gray and semi-gray models for $T_{amb}=20$ °C, $T_{abs}=40$ and 80 °C.

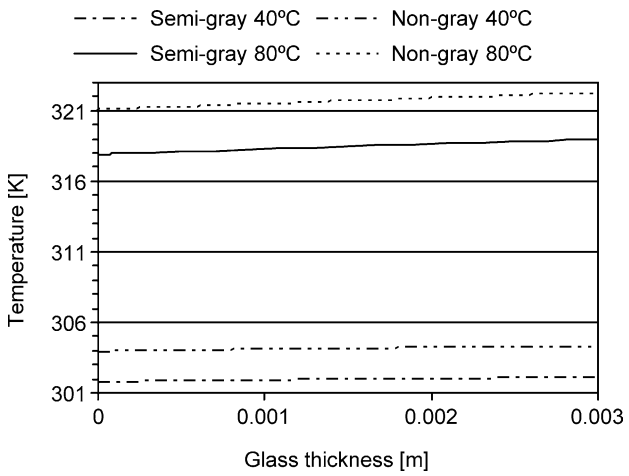

Fig. 6. Temperature distributions within a clear glass cover layer using non-gray and semi-gray models for $T_{amb}=20$ °C, $T_{abs}=40$ °C and 80 °C.

case of semi-gray model is a bit higher than that obtained by the non-gray one at low temperature of the absorber, while, at high temperature of the absorber the steady heat fluxes are almost equal.

Fig. 6 shows the distribution of the temperature through the glass cover. The result shows that the temperature distributions within the glass cover calculated by the non-gray model are higher than those obtained by the semi-gray one at low and high T_{abs}. This is due essentially to the strong absorption, high value of k, within the glass layer when using the non-gray model.

Fig. 7 shows the ratio R, defined as the rate of the CPU time consumed by the SGCL model to the CPU time consumed by NGCL160b model, and the relative deviations of the steady heat fluxes and the average glass cover temperatures in case of SGCL model from the non-gray one. The figure shows that the CPU times are considerably reduced to 4

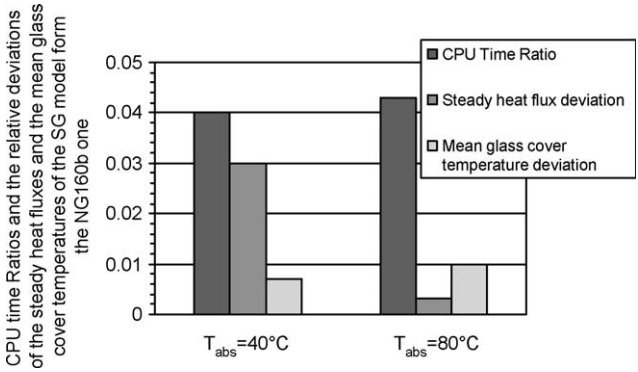

Fig. 7. Comparison of CPU time ratios and relative deviations of the steady heat fluxes and mean temperatures of a clear glass cover calculated using semi-gray model from non-gray one.

and 4.3% for T_{abs} equals to 40 °C and 80 °C, respectively. The relative deviation of the steady heat fluxes when using SGCL from the non-gray one are 3 and 0.3% for 40 °C and 80 °C of T_{abs}, respectively. The relative deviation of the average glass cover temperatures in case of SGCL model from the non-gray one are 0.7 and 1% for T_{abs} equals to 40 °C and 80 °C, respectively. Therefore, it can be concluded that SGCL model is suitable for a rapid calculation with the accuracy still being satisfactory.

3.2. Comparison between the present and classical studies

Fig. 8 shows the comparison of the average glass cover temperatures obtained in the present study with those obtained with the iterative method for different mean absorber temperatures. The comparison shows good agreement, although at high temperature of the absorber the difference becomes larger (around 3 °C), due to the linearity of the heat loss coefficient U_t in case of classical iterative method.

In the present study, the instantaneous efficiency of solar collector is calculated in steady state by dividing the energy that reaches the absorber by the solar radiation flux that falls on the surface of the glass cover, and compared with the classical approach in which the top loss coefficient U_t is assumed to be a linear function of the temperature difference between the plate and the surroundings. The energy that reaches the plate absorber is obtained by multiplying the steady heat flux through the glass cover by the plate absorptivity (taken equal to 0.95).

Fig. 9 shows the instantaneous efficiencies curves obtained in the present study with that obtained using Klein model versus ratio of temperature difference ($T_{abs} - T_{amb}$) to the solar radiation rate (I) for different values of the average plate absorber temperatures with the wind speed velocity taken equal to 1.5 m s^{-1}. The shape of the efficiency curve obtained in the present study is not linear. However, the classical approach assumes

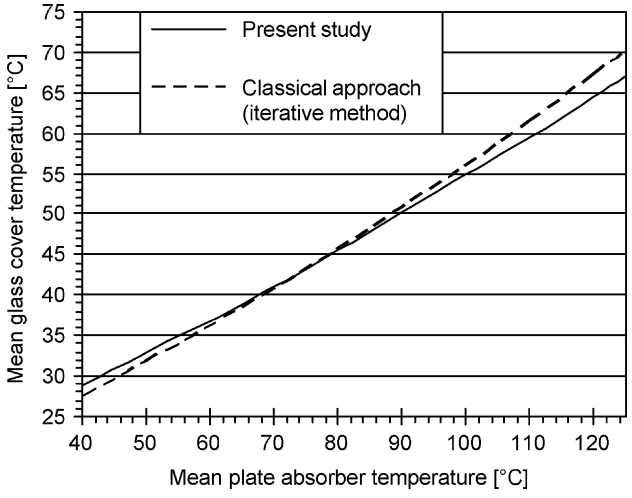

Fig. 8. Average glass covers temperatures obtained by the present study and by the iterative method versus mean plate absorber temperature (clear glass).

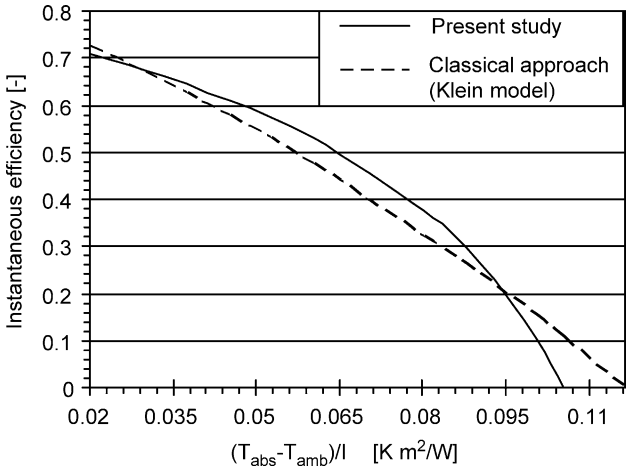

Fig. 9. Solar collector instantaneous efficiencies obtained by the present study and by the classical method (using Klein model) versus mean plate absorber temperature.

the linearity of the overall heat loss from the absorber to the surroundings. In consequence of this assumption, normal flat-plate collector test results are presented as a linear regression of instantaneous efficiency as a function of a ratio of temperature difference to the instantaneous solar radiation rate [8]. In reality, the heat loss from the solar collector is a combination of convection and radiation and is highly non-linear [7].

The efficiency of the solar collector used in low temperature service (up to 50 °C above ambient) can be expressed in linear relation between the average absorber and the ambient temperatures. Physically, this means that the net radiative exchange between the collector and the surroundings is small compared with the convective exchange [2].

The stagnation point is the x intercept of the efficiency curve. The stagnation temperature T_{stag} of the solar collector obtained in the present study is 125 °C (see Fig. 9). Using Klein model, T_{stag} is found to be equal to 136 °C (see Fig. 9). This difference is due essentially to the non-linearity of the emissive power emanating from the plate absorber at high temperature. However, one can see that when the radiation is the dominant heat exchange compared with the convective term, the profile of the efficiency is not straight line.

3.3. Low-iron glass

The optical constants n and k of low-iron material are plotted in Fig. 3 covering the range of interest from 0.3 to 300 μm. The simulation has been carried out using non-gray model (NGLI160b). However, the CPU time was found to be prohibitively long. Therefore, a semi-gray model SGLI has been proposed for rapid computation. Fig. 10 shows the optical constants n and k of low-iron glass in case of semi-gray model.

Fig. 11 shows the steady heat fluxes through the low-iron glass cover obtained both with NGLI160b and SGLI models at 40 °C and 80 °C of the mean absorber plate temperature (T_{abs}). At low temperature of the absorber (40 °C), the steady heat flux

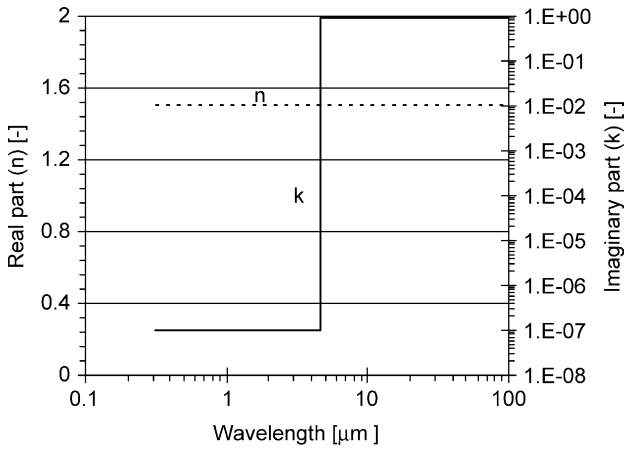

Fig. 10. Real part (n) and imaginary part (k) of the complex refractive index of low-iron glass cover, semi-gray model.

obtained in case of SGLI model is slightly higher than that obtained with NGLI160b one. At high temperature of the absorber (80 °C), the steady heat flux obtained with NGLI160b model is slightly higher than that obtained with SGLI one.

Fig. 12 shows the temperature distributions through the low-iron glass cover. The result shows that the temperature distributions within the glass cover calculated by the NGLI160b model are higher than those obtained with SGLI one at low and high mean temperatures of the absorber. This is essentially due to the strong absorption (high value of k) within the glass layer when using NGLI model.

Fig. 13 shows the ratio R, which is defined as the rate of the CPU time consumed by the SGLI model to the CPU time consumed by NGLI160b one, and the relative deviations of the steady heat fluxes and the average glass cover temperatures in case of SGLI model from the NGLI one. The figure shows that the CPU times are considerably reduced

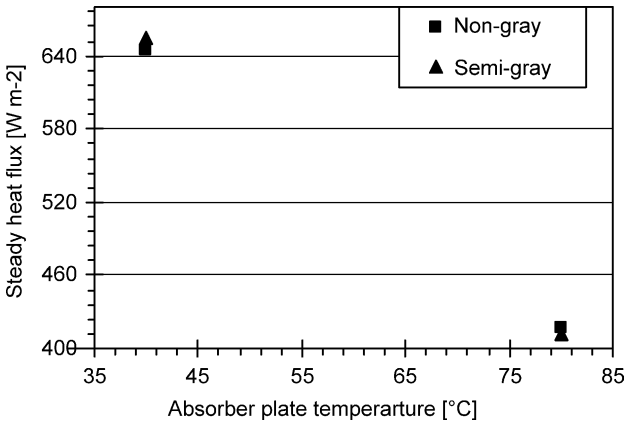

Fig. 11. Steady heat fluxes through the low-iron glass cover using non-gray models for T_{abs} equal to 40 °C and 80 °C.

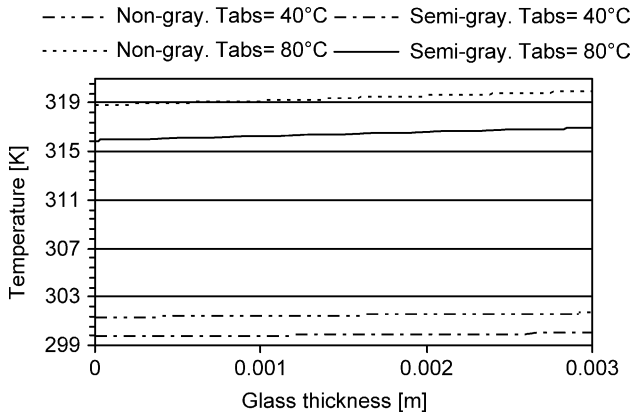

Fig. 12. Temperature distributions with low-iron glass cover layer using non-gray models for T_{abs} equal to 40 and 80 °C.

to 3.1 and 4.1% for T_{abs} equals to 40 °C and 80 °C, respectively. The relative deviation of the steady heat fluxes when using SGLI from the NGLI160b one are 1.7 and 1.3% for 40 °C and 80 °C of T_{abs}, respectively. The relative deviation of the average glass cover temperatures in case of SGLI model from the NGLI160b one are 0.5 and 0.9% for T_{abs} equals to 40 °C and 80 °C, respectively. Therefore, it can be concluded that SGLI model is suitable for a rapid calculation with the accuracy still being satisfactory.

3.4. Comparison between results obtained using clear and low-iron glasses with SG models

Fig. 14 shows the steady heat fluxes obtained with semi-gray models for both clear and low-iron glasses in term of the mean absorber temperature. In case of low-iron glass, the steady heat fluxes are higher than those obtained with clear glass. This is due to the low

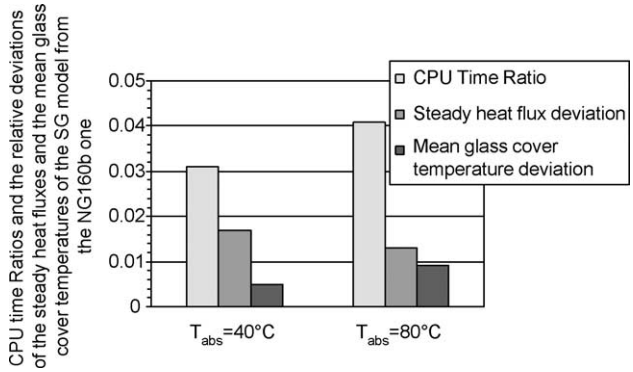

Fig. 13. Comparison of CPU time ratios and absolute deviations of the steady heat fluxes and mean temperatures of low-iron glass cover calculated using semi-gray model from non-gray one.

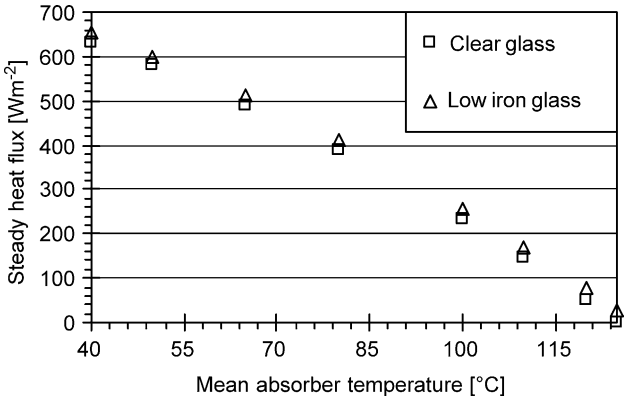

Fig. 14. Steady heat fluxes obtained with semi-gray models for both clear and low-iron glass covers as a function of the mean absorber temperature.

value of k in short wavelength in case of low-iron glass. Therefore, for strong absorption (case of clear glass), the amount of the heat flux through the glass is reduced.

Fig. 15 shows the mean glass cover temperature for both clear and low-iron glasses as a function of T_{abs}. One can see that in case of clear glass the mean glass cover is higher than that obtained with low-iron glass.

Fig. 16 presents the instantaneous efficiencies of the solar collector with both clear and low-iron glass covers. It has been shown in Fig. 9 that the efficiency curve was found to be not linear in shape, due to the non-linearity of the convective and radiative heat losses from the collector. The result shows that the solar collector with low-iron glass has a higher efficiency, because the amount of the steady heat flux traveling through the glass cover is higher in case of low-iron glass.

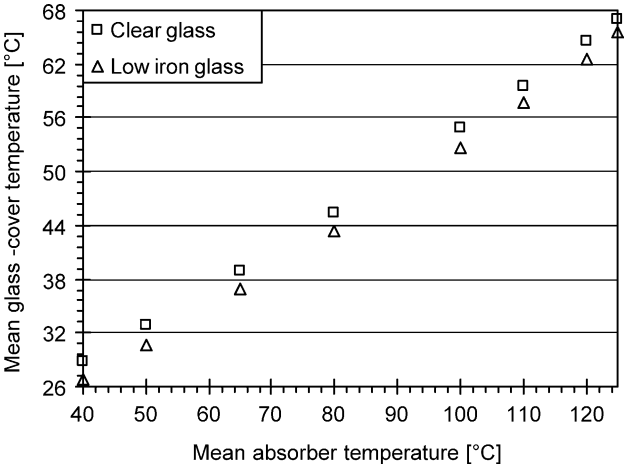

Fig. 15. Mean glass cover temperatures obtained with semi-gray models for clear and low-iron glass cover in term of mean plate absorber temperature.

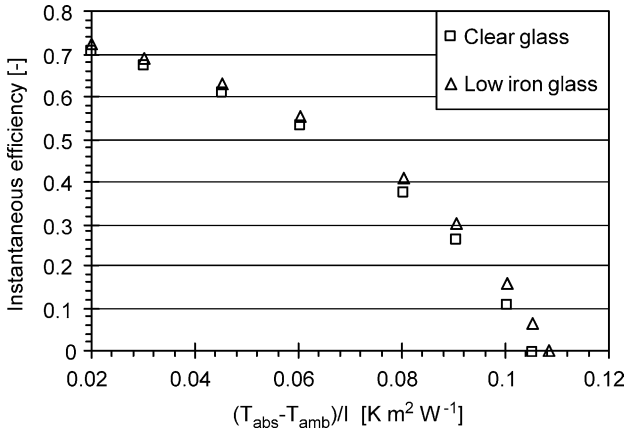

Fig. 16. Instantaneous efficiencies of the solar collector using clear and low-iron glass cover versus $(T_{abs} - T_{amb})/I$.

4. Concluding remarks

Accurate modeling of solar collector system using a rigorous radiative model is applied for the glass cover which represents the most important component of the system and greatly affects the thermal performance. The non-gray calculation procedure taking into account the absorption and emission within the glass covers (clear and low-iron) using the radiation element method by ray emission model is applied. The following points summarize the results obtained in the present paper.

The CPU times consumed in case of non-gray models with 160 bandwidths were found to be prohibitively long for both clear and low-iron glasses. Therefore, rapid semi-gray models have been proposed and found to be suitable for quick simulation with accuracy still being satisfactory.

The comparison of the glass cover mean temperature obtained in the present study in case of clear glass with those obtained using the classical iterative method shows a good agreement, although the difference becomes larger at high temperature of the absorber, due to the linearity of the heat loss coefficient U_t in case of classical iterative method.

The profiles of the efficiencies curves obtained in the present study were found to be not linear in shape for both clear and low-iron glasses. Indeed, the heat loss from the collector is a combination of convection and radiation and highly non-linear.

The instantaneous efficiency of the system is higher in case of low-iron glass cover.

References

[1] Duffie JA, Beckman WA. Solar energy thermal process. New York: Wiley; 1974 [chapters 4–7].
[2] Howell JR, Bannerot RB, Vliet GC. Solar-thermal energy system. Analysis and design. New York: McGraw-Hill; 1982 [chapters 2–5].

[3] Bird RE, Riordan C. Simple solar spectral model for direct and diffuse irradiance on horizontal and tilted planes at earth's surface for cloudless atmosphere. Journal of Climate and Applied Meteorology 1986;25: 87–97.
[4] Rubin M. Optical properties of soda lime silica glasses. Solar Energy Mater 1985;12:275–88.
[5] Maruyama S, Aihara T. Radiation heat transfer of arbitrary three-dimensional absorbing, emitting and scattering media and specular and diffuse surfaces. J Heat Transfer 1997;119:129–36.
[6] Maruyama S. Radiative heat transfer in anisotropic scattering media with specular boundary subjected to collimated irradiation. Int J Heat Mass Transfer 1998;41:2847–56.
[7] Agarwal VK, Larson DC. Calculation of the top loss coefficient of a flat-plate collector. Solar Energy 1981; 27:69–77.
[8] Cooper PI, Dunkle RV. Anon-linear flat-plate collector model. Solar Energy 1981;26:133–40.